Ind. J. Pharm. Edu. Res., 2026; 60(2s):s776-s793.
https://www.ijper.org

Original Article

Optimizing Tumor-Targeting Drug Delivery of Potent Anti-Cancer Drug Using Doe-Guided Solid Lipid Nanoparticle Formulation: *In vitro* Cell Line Studies and Histopathological Analysis

Ramineni Sunitha[1], Praveen Sivadasu[1,*], Pathange Bharghava Bhushan Rao[2], Raghavendra Kumar Gunda[3]

[1]Department of Pharmacy, Koneru Lakshmaiah Education Foundation, Green Fields, Vaddeswaram, Andhra Pradesh, INDIA.
[2]Department of Pharmaceutics, A. M. Reddy Memorial College of Pharmacy, Petlurivaripalem, Narasaraopet, Andhra Pradesh, INDIA.
[3]Department of Pharmaceutics, Narasaraopeta Institute of Pharmaceutical Sciences (Autonomous), Narasaraopet, Palnadu, Andhra Pradesh, INDIA.

ABSTRACT

Background: Lapatinib Ditosylate emerges as a notable contender; it functions as potent selective dual tyrosine kinases ErbB-2 and EGFR inhibitor and it is a class-II drug. The present work focuses on the development of Lapatanib loaded SLNs for targeting Breast Cancer. **Materials and Methods:** By employing Box-Behnken design, this study evaluates the impact of three key factors on the formulation of Lapatinib-loaded SLNs: the drug-to-lipid ratio (VX1), the concentration of Labrafil (lipid phase surfactant) (VX2), and the sonication time (VX3). The outcomes of this research will focus on two primary responses: the average particle size (Y1) and the % EE (Y2). The prepared SLNs were studied for percent drug content, PSD, % EE, zetapotential, *in vitro* drug release studies, Invitro screening of anticancer efficacy by cell line studies and *in vivo* studies through Histopathological studies. **Results:** From research findings, the optimal formulation was selected by achieving encapsulation efficiency exceeding 85% and particle sizes under 250 nm; additionally, it was observed that the drug release rate was enhanced at pH 5.0 compared to pH 7.4, while invitro studies demonstrated that LP-SLNs exhibited an IC_{50} nearly 6 times lower against SKBr3 cells compared to the LS formulation, signifying a markedly superior anticancer efficacy, further supported by histopathological examinations revealing that LP-SLNs significantly mitigated liver toxicity. **Conclusion:** This comprehensive investigation not only reaffirms the utility of SLNs in improving the delivery and effectiveness of anticancer agents but also accentuates the potential of creating tailored formulations that address the complex challenges inherent in oncological treatments.

Keywords: Lapatanib, SLNs, Box Behnken Design, Cell Line Studies, Histopathological Studies and Screening of Anticancer Efficacy.

Correspondence:
Dr. Praveen Sivadasu
Department of Pharmacy, Koneru Lakshmaiah Education Foundation, Green Fields, Vaddeswaram, Andhra Pradesh, INDIA.
Email: praveen.sivadasu399@gmail.com

Received: 02-12-2025;
Revised: 12-01-2026;
Accepted: 24-02-2026.

INTRODUCTION

Cancer is a complex disease that emerges from the unchecked proliferation of cells within the body. This uncontrolled growth is primarily attributed to the cells' inability to properly undergo a natural process known as apoptosis, which is essentially programmed cell death. When cells fail to die as they should, they accumulate and form tumors, leading to the progression of cancerous conditions. Several studies and literature reviews have documented these cellular mechanisms, highlighting their critical role in cancer development.[1-7] Some of the most commonly diagnosed cancers around the world include breast cancer, lung cancer, prostate cancer, and colorectal cancer. Each of these types has unique characteristics and challenges in terms of treatment and management, making research into their pathophysiology and treatment options vital.

In recent years, the development of lipid-based DDS has gained attention in cancer therapy. One such system is SLNs, which are sub-micron-sized carriers made from lipid components that are generally considered physiologically safe. SLNs can encapsulate a variety of drugs, whether lipophilic (fat-soluble) or hydrophilic (water-soluble), enabling a versatile approach to drug formulation.[8-10]

A notable example of a targeted cancer therapy is Lapatinib Ditosylate. This drug acts as a selective and potent inhibitor of the ErbB-2 and Epidermal Growth Factor Receptor (EGFR) tyrosine

DOI: 10.5530/ijper.20261953

kinases, which play a crucial role in many cellular processes, including cell growth and survival.[11-13] It belongs to Class II.[14-16]

To enhance the properties of Lapatinib Ditosylate and improve the bioavailability of the drug when delivered via SLN systems, researchers have undertaken the preparation of lipid nanoparticles. This approach has led to improved encapsulation efficiency for the drug, as well as enhanced targeting to tumor sites through passive mechanisms, thus potentially increasing the therapeutic effectiveness of the treatment.[17,18] By bridging advances in nanoparticle technology with cancer pharmacotherapy, there is a promising avenue for improving patient outcomes in cancer treatment.

MATERIALS AND METHODS

Materials

Lapatinib was procured as a gift sample from Lupin Pharma Limited. Excipients like, Labrafac Lipophile WL1349, Precirol ATO5, Compritol ATO 888 were obtained from Gattefosse, France. Other materials such as Tween-80, Tween-20, Span-20, and Labrafile, Glucirol, Chromophore were purchased from Merck Pvt. Ltd., Mumbai.

Methods

HPLC analytical method development

The HPLC analytical technique was employed to quantify the concentration of LP in plasma samples collected from rats during pharmacokinetic investigations. The HPLC system components included a Rheodyne 7725i manual injector, a 1525 binary HPLC pump, a C18 reverse-phase column (4.6x75 mm; 3.5 µm) from Symmetry®, and a Waters 2998 photodiode array detector, all sourced from Waters, USA. The mobile phase utilized was a mixture of Methanol and Milli-Q water in a ratio of 80:20, with a flow rate set at 1.0 mL/min.[19-23]

The column was kept at a temperature of 30±1°C throughout the procedure. The measurement of LP was conducted at a wavelength of 368 nm. Breeze2 software was used to integrate peak area and determine retention time and was further used for drug content determination. Standard calibration curves in desired media were constructed in range of 500-3000 ng/mL of LP for *in vivo* samples. Typical validation characteristics (specificity, precision, accuracy, linearity range, limit of detection, and limit of quantification) were calculated in method validation to meet the acceptance criteria described in ICH Q2 (R1) guidelines.

Formulation and development of Lapatinib loaded SLN

Solubility study of Lapatinib in various lipids

Compritol 888 ATO, Precirol ATO 5, Emulcire, stearic acid, and glyceryl monostearate were utilized for experimentation. A total of 0.1 g of the drug was introduced into a test tube, to which solid lipid was gradually incorporated in increments of 0.5 g. The required quantity of solid lipid needed to facilitate drug solubilization in its molten state was established.[24-28]

Solubility study of drug in various surfactants

The surfactants chosen for this research included Gelucire 44/14, Labrafil M2125, Labrafil M1944, Tween 20, Tween 80, Span 20, and Span 80. An excess amount of the drug was incorporated into a specified volume of the surfactant systems and mixed for a duration of 2 min. Subsequently, a mechanical shaker was employed for an additional 12 hr to ensure the complete dissolution of the drug. The samples were subsequently subjected to centrifugation at 10,000 rpm for a duration of 15 min. The resulting aliquots of the supernatant from the saturated surfactant systems were then appropriately diluted with methanol and analyzed using UV spectrophotometry at a wavelength of 368 nm.

Study of stability of pre-emulsion

Different pre-emulsions were prepared using drug, lipid (Labrafac LipophileWL1349, Compritol ATO 888 or Precirol ATO 5), lipid phase surfactant (Labrafile or Span 80) and aqueous phase with surfactant (Cremophore EL or Tween 80). These pre-emulsions were prepared with different combinations of lipid phase as well as aqueous phase surfactant (Table 1 (A)) and were kept at ambient temperature for one week to study their stability.

Preparation method of SLN

The method chosen for the preparation of Lapatinib-loaded SLNs was the pre-emulsion technique, which was subsequently followed by probe sonication. In summary, the lipid phase was composed of Lapatinib, lipid, and a surfactant, all maintained at a temperature of 70°C. An aqueous phase was created by dissolving a surfactant in distilled water, with the volume sufficient to yield 50 mL of the final preparation, and subsequently heated to match the temperature of the oil phase. The hot aqueous phase was incorporated into the oil phase, and homogenization was performed at 70°C utilizing a high-speed homogenizer at various speeds for a duration of 30 min.[29]

Experimental design and statistical analysis

Based on stability of pre-emulsion (Table 1(A)) labrafac lipophile WL 1349 (mg) as solid lipid and Labrafile M2125 as surfactant and tween 80 as cosurfactant were selected for further optimization. In simultaneous optimization, the experimentation is conducted prior to the optimization process. This research employed a BBD to develop the formulation of SLNs. Box-Behnken Design (BBD) was selected for its efficiency in requiring fewer experimental runs than Central Composite Design while allowing robust estimation of the interaction and quadratic effects. BBD is particularly suitable for optimizing three formulation variables (drug-to-lipid

ratio, surfactant concentration, and sonication time) with minimal experimental cost and high predictive accuracy.

The lipid was selected based on the solubility and partitioning characteristics of Lapatinib in connection with the lipid. Surfactants for both the aqueous phase and the lipid phase were chosen based on the stability of the dispersions created with various surfactants. 3 factors, the drug: lipid ratio (VX_1), concentration of Labrafile (lipid phase surfactant) (VX_2) and sonication time (VX_3) were used in the design and the responses were the average PS (Y_1) and % EE (Y_2). The three factors that could influence the designed characteristics of the nanoparticle formulation were adjusted across three levels and organized in accordance with a BBD (Table 1).[30-33]

Evaluation of optimized batch of Lapatinib loaded SLN

Characterization of optimized batch of Lapatinib loaded SLN

PSA and PDI

The average particle size and polydispersity index of the optimized batch of drug-loaded SLNs were determined using a particle size analyzer that employs the dynamic light scattering technique.[34-37] The SLN formulations were dispersed in distilled water at correct concentrations. All measurements were performed in triplicate. The PDI indicates the width of the size distribution.

Determination of %EE and Drug Loading (DL)

The EE of optimized batch of drug loaded SLN was calculated by centrifugation method as described in section.

The %EE and DL were calculated by using equation.

$$DL = \frac{W\ initial\ drug - W\ free\ drug}{W\ lipid} \times 100$$

In this context, Winitial drug refers to the weight of the initial drug incorporated into the formulation, Wfree drug denotes the weight of the free drug present in the supernatant, and W lipid indicates the total weight of lipid within the formulation.

Zeta potential

The zeta potential of the optimized batch of drug-loaded Solid Lipid Nanoparticles (SLN) was assessed using a zeta potential analyzer that operates on the principle of Laser Doppler Micro-electrophoresis. An electric field was introduced to the particle dispersion, causing the particles to move at a velocity that correlates with their zeta potential. This velocity was assessed through a laser interferometric technique, which facilitates the determination of electrophoretic mobility, subsequently allowing for the calculation of the zeta potential.

SEM

The surface morphology of the optimized SLNs formulation was examined using a field emission scanning electron microscope at a temperature of 25±2°C. The SLNs dispersion was applied to aluminum foil and allowed to air dry for 24 hr. Subsequently, it was analyzed at a magnification of 3000× with an accelerating voltage of 10kV.

FTIR

FTIR spectroscopy was performed on both the pure drug and the optimized batch of drug-loaded Solid Lipid Nanoparticles (SLNs). A sample of the dry drug was mixed with potassium bromide (IR grade) in a ratio of 1:100. This mixture was then pressed using a hydraulic press to form a pellet under a pressure of 10 tons. The resulting pellets were scanned using the FTIR instrument over a wavenumber range of 4000 to 400 cm^{-1}, followed by a spectral analysis. The acquired spectrum was subsequently compared with the standard vibrational frequencies of Lapatinib.

DSC

DSC analyses were carried out on both the pure drug and the optimized formulation of drug-loaded Solid Lipid Nanoparticles (SLNs). These measurements were performed using a differential scanning calorimeter linked to a computerized data station. The sample was weighed and placed in a sealed aluminum pan with a perforated lid, then heated at a scanning rate of 10°C/min over a temperature range of 50 to 300°C, while maintaining a nitrogen flow rate of 40 mL/min.

X-ray diffraction

The X-ray diffraction pattern of the pure drug and the optimized batch of drug-loaded SLNs was obtained using an X-ray diffractometer.

In vitro evaluations

In vitro drug release studies

A dialysis membrane bag, pre-soaked and with a molecular weight cut-off of 14 kDa (Fisherbrand), was filled with 1 mL of the optimized LP dispersion, which corresponds to 2 mg of LP, and both ends were securely sealed. In the case of the lyophilized form, the powder was re-dispersed in 1 mL of deionized water prior to being sealed within a dialysis bag. The dialysis bag was subsequently placed into 50 mL of release media (PBS at pH 7.4 and PBS at pH 5.0), which was kept at a temperature of 37±0.5°C while being stirred at a speed of 100 RPM. To maintain sink conditions and facilitate drug release, 0.5% Tween 80 was incorporated into the media.[38]

In vitro Screening of anticancer efficacy

Cell Culture

The SKBr3 cell line was chosen due to its overexpression of HER2, making it highly suitable for evaluating the efficacy of Lapatinib, a HER2-targeting agent. The SK-BR-3 cell line serves as a crucial model for HER2+ breast cancers, impacting approximately one

in five patients with breast cancer. This cell line is characterized by significant genetic rearrangement, though much of this variation occurs in complex and repetitive regions that could be overlooked in reports. McCoy's 5A medium, enriched with 100 U/mL of penicillin, 10% fetal bovine serum, and 100 mg/mL of streptomycin, was employed for the cultivation of SKBr3 cells. The cells were maintained at 37°C in an atmosphere containing 5% CO_2. For *in vitro* screening purposes, the cells were seeded as required following trypsinization.

Cytotoxicity assay

MTT assay of LP-SLNs was performed, to assess its cytotoxicity. 96-well culture plates were used for seeding the cells (density of2×104 cells/well) and cultured for a period of 24 hr. Next day, serial dilutions of LP-SLNs and LS were added to the cultured cells; those were previously in range of 0.05 to 100 µg/mL. MTT assay was then completed as per protocol. Obtained data was analysed to calculate IC_{50} values and percent cell viability by using Graph Pad Prism software. Non-cancerous cell lines were not included in the current study.

In vitro anti-cancer efficacy studies

The changes in the morphology of SKBr3 cells before and after treatment were observed using inverted microscope. The cells (104 cells per well) were seeded in a 24-well culture plate and subjected to treatment with a placebo micelle, LP Solution (LS), and LP-SLNs (10 µg of LP/mL) for a duration of 24 hr. The cells were subsequently rinsed three times with PBS and then fixed in 4% paraformaldehyde in PBS (pH 7.4) for a duration of 15 min at room temperature. The fixed cells were subjected to a second wash with PBS and subsequently mounted onto glass slides. Following this, the slides were examined using an inverted light microscope.[39-44]

In vivo evaluations

Histopathological studies

The lapatinib was reported to show hepatotoxicity and thus, histochemical and pathological studies were performed. Briefly, the liver tissues obtained from each group were preserved in 10% (v/v) formalin saline and subsequently subjected to standard histopathological techniques. The paraffin-embedded specimens were sectioned into 5 mm slices and stained with Hematoxylin and Eosin (H&E) for histopathological assessment. The histological examination was performed under microscope after H&E staining.[45-50]

RESULTS AND DISCUSSION

HPLC Method for Lapatinib

Standard stock solutions of lapatinib and gemcitabine hydrochloride were carefully prepared to enable a thorough analytical evaluation of these important cancer treatment drugs. Specifically, 25 mg of each compound was dissolved separately in 25 m of a solvent mixture of acetonitrile and water in a 50:50 v/v ratio, resulting in concentrated stock solutions with a final concentration of 1 mg/mL. From these stock solutions, working standard solutions of lapatinib were prepared ranging from 2 to 60 µg/mL with gemcitabine hydrochloride consistently maintained at an internal standard concentration of 5 µg/mL. The mobile phase was utilized as the solvent for these working standards (see Figure 1), allowing for accurate measurements in subsequent analyses. To determine the relationship between lapatinib concentration and the corresponding analytical response, a calibration curve was created using linear regression, yielding the equation y=0.025949x+0.054673, where y represents the detector response and x denotes the concentration of lapatinib. The strong correlation coefficient (R^2 = 0.996408) reflects the high reliability and robustness of the analytical method. In terms

Table 1: Box-Behnken design accompanied by relevant formulations.

Formula CODE	VX_1	VX_2	VX_3	VX_1	VX_2 (%)	X_3 (min)
L_1	0	-1	-1	1:2	1	10
L_2	0	+1	+1	1:2	3	30
L_3	-1	0	+1	1:1	2	30
L_4	-1	-1	0	1:1	1	20
L_5	0	-1	+1	1:2	1	30
L_6	+1	0	-1	1:3	2	10
L_7	+1	-1	0	1:3	1	20
L_8	0	0	0	1:2	2	20
L_9	+1	0	+1	1:3	2	30
$^L10$	-1	0	-1	1:1	2	10
$^L11$	+1	+1	0	1:3	3	20
$^L12$	0	+1	-1	1:2	3	10
$^L13$	-1	+1	0	1:1	3	20

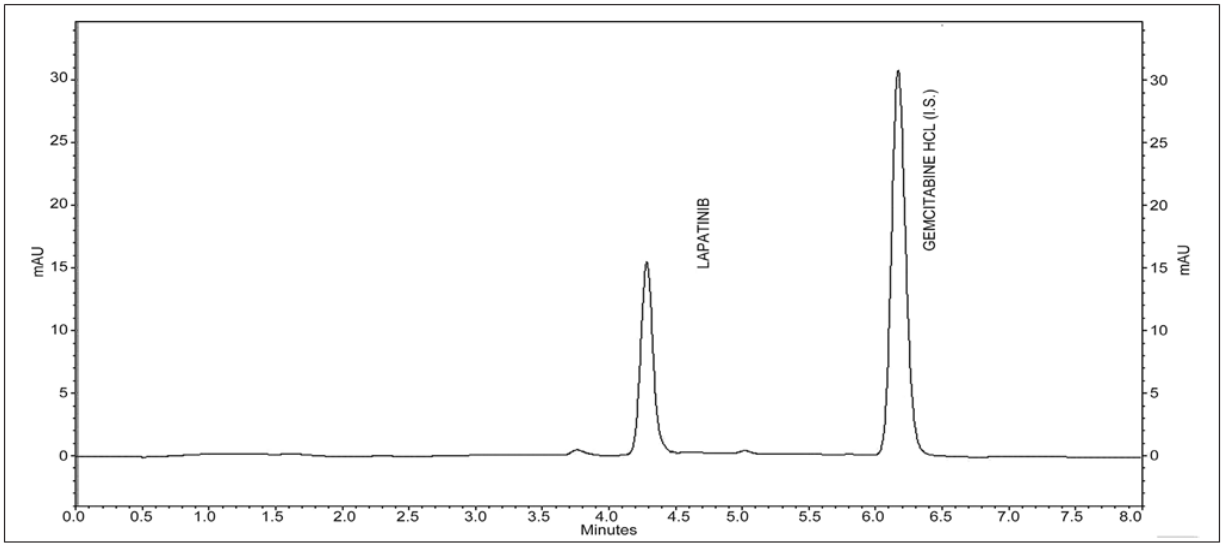

Figure 1: HPLC Chromatogram of Lapatinib with IS Gemcitabine HCl.

of sensitivity, the Limits of Detection (LOD) and Quantitation (LOQ) were systematically evaluated by analyzing three distinct concentrations within the calibration range, each performed in triplicate. Results indicated that the method's accuracy demonstrated a commendable agreement between true values and experimental outcomes, affirming its validity. Additionally, the percentage Relative Standard Deviation (% RSD) values for both intra-day and inter-day precision tests were consistently below 3%, indicating exceptional repeatability and intermediate precision of the analytical technique.

Solubility study of Lapatinib in various lipids & Surfactants

In this study Solubility of Lapatinib in 5 chemically different lipids with different HLB values were screened to select a lipid on the basis of solubility of drug. The solubility of drug in lipids was observed in the following order: Labrafac Lipophile WL1349 > Compritol 888ATO > Precirol 5ATO > Stearic acid. These results highlight the significant variation in solubility profiles among different lipids, influenced by their chemical structures and HLB values. The findings suggest that Labrafac Lipophile WL1349 may be the most suitable lipid for potential formulations aimed at enhancing the bioavailability of Lapatinib, while the other lipids may have varying degrees of efficacy based on their solubility capacities. Further studies could explore the implications of these solubility profiles for optimizing drug delivery systems and improving therapeutic outcomes for patients using Lapatinib.

Solubility study of the drug in various surfactants

Among the various types of surfactants studied, the results from solubility analyses revealed that Lapatanib, a pharmaceutical compound, exhibits a notably high level of solubility when formulated with Labrafil M2125 and Tween 80. This observation suggests that these specific surfactants can effectively enhance the dissolution properties of Lapatanib, which is an important characteristic for its potential applications in drug delivery and formulation development. Labrafil M2125, a self-emulsifying mixture that aids in the solubilization of lipophilic compounds, along with Tween 80, a widely used non-ionic surfactant known for its surfactant properties and ability to improve the stability of emulsions, together contribute positively to the solubility profile of Lapatanib. This information is crucial for researchers and formulators looking to optimize the delivery of Lapatanib, as better solubility can lead to improved bioavailability and efficacy in therapeutic applications.

Study of stability of pre-emulsion

The findings from this comprehensive study highlight several important observations regarding the solubility characteristics of the drug in question, suggesting significant implications for its formulation and potential therapeutic applications. It was observed that the drug demonstrates a markedly high solubility when combined with lipid components such as Labrafac, in addition to surfactants such as Labrafine and Tween 80. These solubility traits are not merely technicalities; they play a crucial role in influencing the formulation of the drug and its overall effectiveness within the delivery system designed for its administration. Furthermore, when emulsions were meticulously prepared using these specific lipid and surfactant combinations, they exhibited exceptional stability across various assessments performed during the study. This enhanced stability is a significant advantage, indicating that the emulsion can maintain its structural integrity and efficacy over extended periods. Such stability is essential for ensuring consistent therapeutic performance, which is vital for patient safety and the effectiveness of the drug when administered. The observations from this study suggest that employing Labrafac, Labrafine, and Tween 80 as key components provides a robust foundation for the formulation of Solid Lipid Nanoparticles (SLNs). The selection

of these ingredients is not arbitrary; it is deeply rooted in their unique capacity to enhance both the solubility of the drug and the stability of the resulting formulation. This strategic choice not only optimizes the pharmacokinetic properties of the drug but also paves the way for the development of more effective drug delivery systems in future applications, ultimately improving patient outcomes and expanding the therapeutic potential of the drug in question. Overall, the insights gained from this research underscore the importance of carefully selecting formulation components based on their solubility and stability characteristics. By advancing our understanding of how different ingredients interact with the drug and contribute to its delivery efficacy, we can better tailor drug formulations to meet clinical needs and enhance treatment success rates. Consequently, the findings of this study hold promise for future innovations within the field of pharmaceutical sciences, particularly in the design of delivery systems that leverage the unique properties of lipid-based formulations.

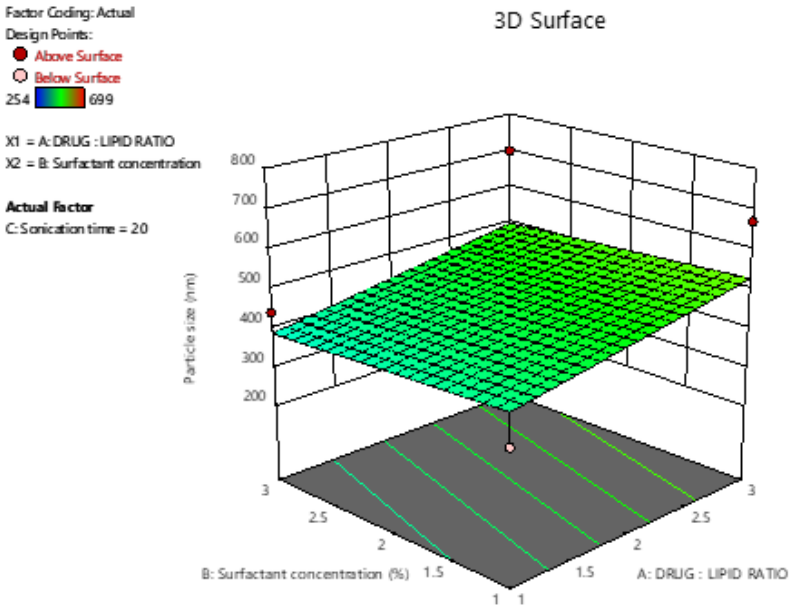

2A

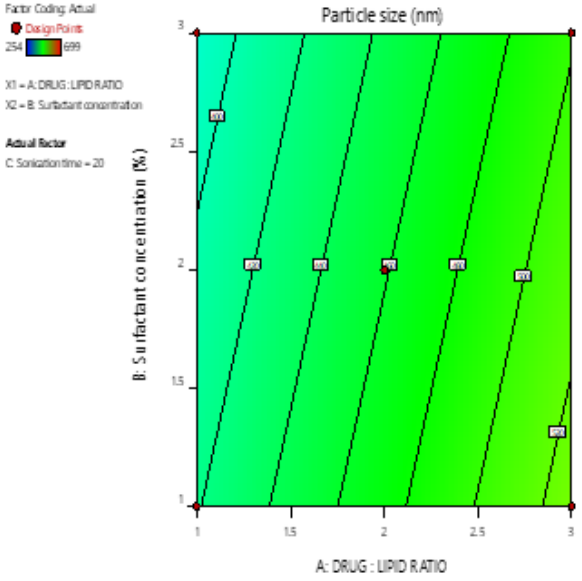

2B

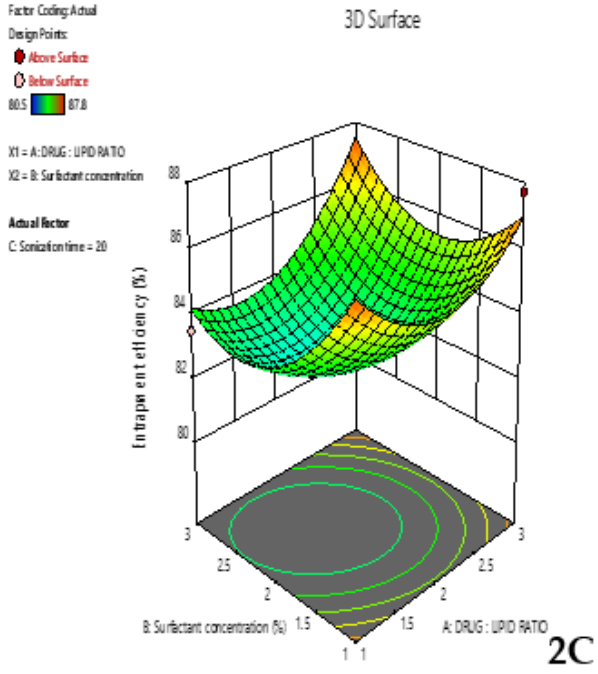

2C

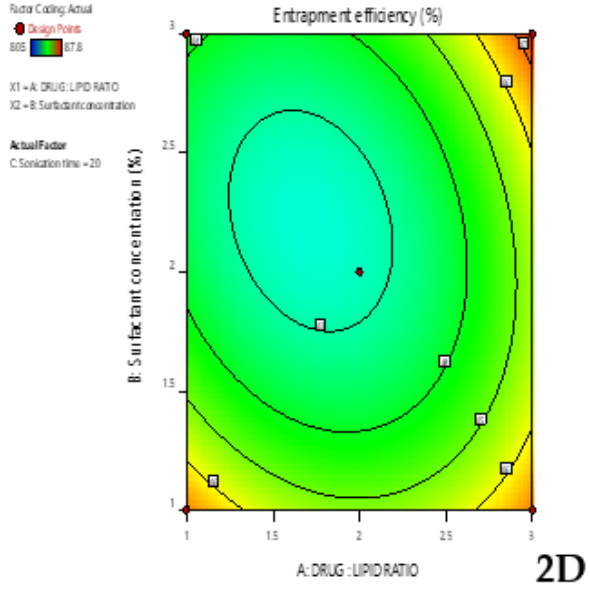

2D

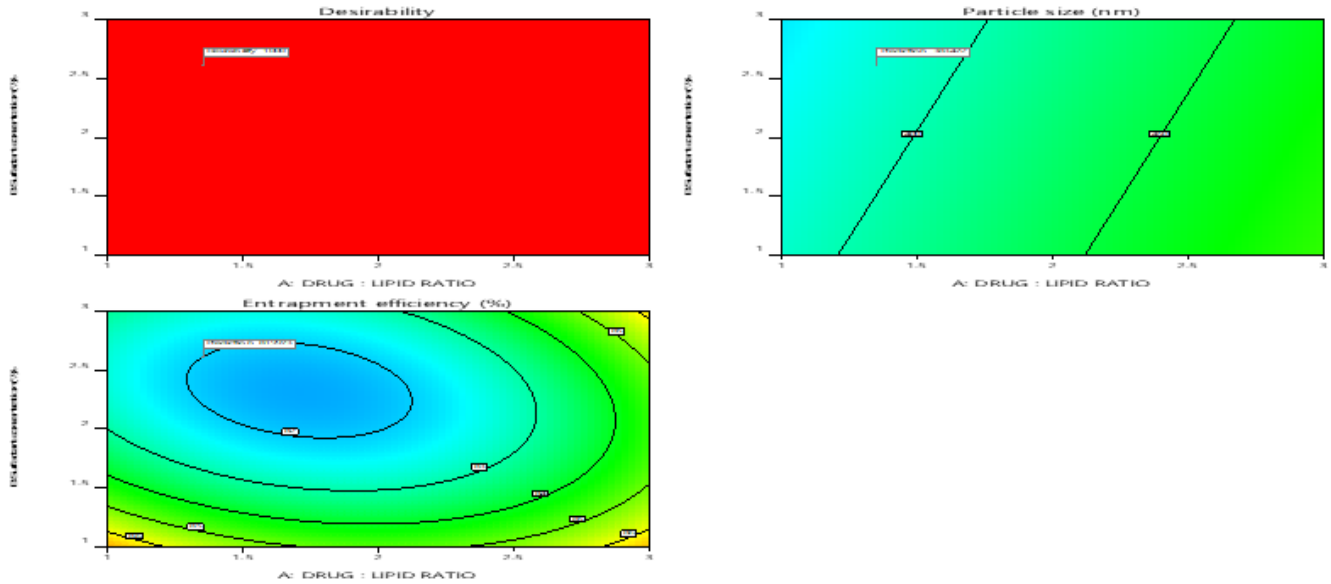

2E

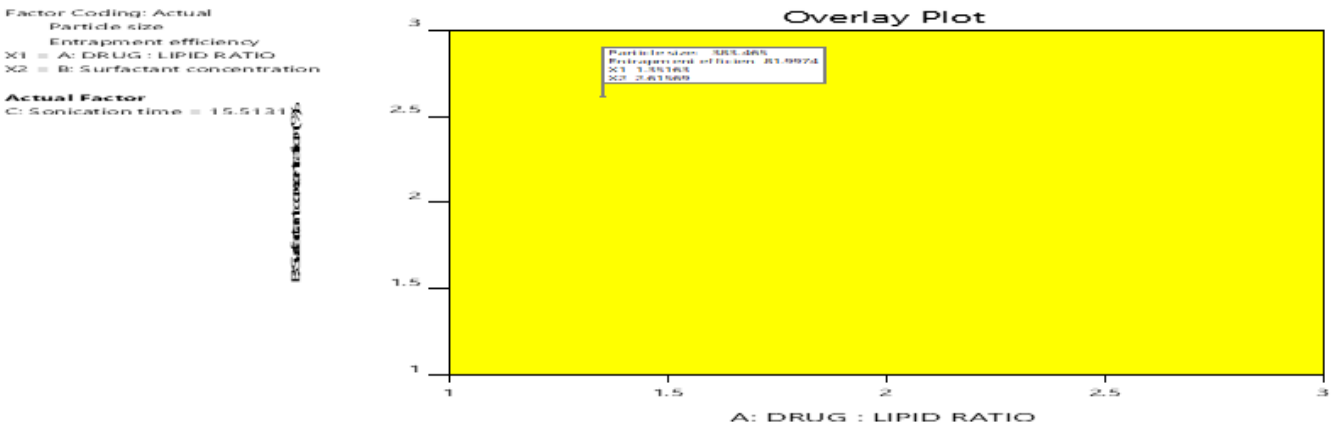

2F

Figure 2: 2A-3D-response surface graphs plots, 2B-2D Counter Plots for Particles Size, 2C- 3D-response surface graphs plots, 2D-2D Counter Plots for % EE. 2E-Desirability Plots and 2F-Overlay plot.

Experimental design and statistical analysis

The coefficients of the polynomial equations produced by Design Expert 12 for the particle size and percentage Encapsulation Efficiency (% EE) of the Lapatanib-loaded SLNs dispersion are presented in (Table 2). A total of nine coefficients, labeled from a to i, were computed, with k representing the intercept.

$$Y=k+aX1+bX2+cX3+dX1X2+eX1X3+fX2X3+gX12+hX2+iX32 \ldots.$$

The equation can be utilized to derive estimates of the responses, as demonstrated in Table 3. The second-order polynomial equation that describes the relationship between the response of particle size (Y1) and the independent variables is presented in Table 3. As Table shows, the ANOVA test indicates that among the studied independent variables examined, the interactions of X_1X_3 and X_2X_3 and quadratic effect of X_2 ($p<0.05$). The negative coefficients of X_2 and X_3 indicate that particle size of SLN decreases with increasing levels of surfactant concentration and sonication time. This relationship is succinctly summarized in Table 3, which provides both visual and numerical representations of the data. Understanding the size of the particles is critical, as it plays a significant role in the cellular absorption of drug-loaded Solid Lipid Nanoparticles (SLNs) by absorptive enterocytes. The size of these nanoparticles can greatly impact their effectiveness in drug delivery systems, determining how effectively they can be taken up by cells and how well they can release their cargo within the cellular environment. Moreover, it is noteworthy that the duration of sonication, a process used to disperse and reduce particle size, has a profound effect on the final size of the particles.

Table 1 (A): Composition of trial batches for pre-emulsion stability.

Ingredients /Batch	Drug (mg)	Labrafac Lipophile WL1349 (mg)	Compritol ATO 888 (mg)	Precirol ATO5 (mg)	Span 20 (%)	Labrafile M2125 (%)	Cremophore EL (%)	Tween 80 (%)
LD1	250	500	-	-	3	-	3	-
LD2	250	500	-	-	3	-	-	3
LD3	250	500	-	-	-	3	3	-
LD4	250	500	-	-	-	3	-	3
LD5	250	-	500	-	3	-	3	-
LD6	250	-	500	-	3	-	-	3
LD7	250	-	500	-	-	3	3	-
LD8	250	-	500	-	-	3	-	3
LD9	250	-	-	500	3	-	3	-
LD10	250	-	-	500	3	-	-	3
LD11	250	-	-	500	-	3	3	-
LD12	250	-	-	500	-	3	-	3

As the duration of sonication is extended, a significant reduction in particle size is observed. This phenomenon can be attributed to the generation of cavitational forces that occur during the sonication process. These forces create rapid pressure changes that lead to the formation and collapse of microscopic bubbles. This collapsing action helps facilitate the breakdown of larger lipid droplets into much smaller particles that reach the nanometer scale. Consequently, this reduction in particle size not only enhances the overall distribution of the drug-loaded SLNs but also increases their surface area, which is a crucial factor in improving their interaction with biological membranes. An increased surface area can potentially enhance the absorption efficiency of the nanoparticles, thereby improving the bioavailability of the drug being delivered. Overall, the interplay between sonication duration, particle size, and the resulting biological interactions underscores the importance of optimizing these parameters in the formulation of effective drug delivery systems.

The relationship between the Encapsulation Efficiency (EE) of Solid Lipid Nanoparticles (SLN), denoted as Y2, and several independent variables is mathematically characterized by a second-order polynomial equation, which is detailed in Table 3. This equation captures the complex interplay between the various factors affecting EE in a quantitative manner. To further analyze these influences, an Analysis of Variance (ANOVA) test was conducted. The results from this statistical evaluation demonstrate that among the independent variables considered, only certain interactions between them-specifically the interactions of X1 with X3 and X2 with X3-along with the quadratic effect of X3, showed statistically significant impacts on the encapsulation efficiency, as indicated by a *p*-value of less than 0.05. This suggests that these factors play a critical role in determining how well the solid lipid nanoparticles can encapsulate the active pharmaceutical ingredient. Delving deeper into the findings, the presence of a negative coefficient related to variable X2 implies that as the concentration of Labrafile, a type of emulsifier, increases, the encapsulation efficiency of the SLN tends to decrease. This is a crucial insight, as it indicates that higher levels of this emulsifier do not benefit, and may indeed hinder, the process of drug encapsulation in solid lipid nanoparticles. In stark contrast, the results indicate that a rise in lipid concentration, represented by variable X1, positively influences the encapsulation efficiency. This is primarily because a higher availability of lipid facilitates a greater capacity for drug entrapment within the nanoparticles. The lipid matrix plays an essential role in creating a favorable environment for the drug to be incorporated. However, it is important to note that while increasing lipid concentration can be beneficial, an elevation in the percentage of emulsifier might have unfavorable consequences. Specifically, an excessive amount of emulsifier can lead to dissolution of some of the active pharmaceutical ingredient into the external phase rather than maintaining it within the nanoparticles. This transfer of the drug outside of the lipid matrix can ultimately result in reduced encapsulation efficiency, highlighting the need for a careful balance between lipid and emulsifier concentrations when formulating solid lipid nanoparticles. Overall, these findings underscore the intricate balance required in the formulation process for solid lipid nanoparticles, where both the type and concentration of variables must be optimized to achieve the desired encapsulation efficiency.

The Figures (2A-2F) would have a visualization of effects of the independent variables on the response variables i.e., Particle size and entrapment efficiency. 2D Contour Plots showing the effects of 2 factors on the response variable while holding the 3rd factor to zero or constant. 3D Response Surface Plots showing the effects

of 2 factors on the response variable within the experimental range while holding other factors to zero or constant. Pertubation Plots helps to compare the effects of all factors at a particular point in the design space. For particle size (Y1), the regression equation had an $R^2 = 0.996$, indicating a highly predictive model. The manuscript shows that X1X3, X2X3, and $X2^2$ significantly impacted particle size and EE ($p<0.05$) as detailed in Table 3. Figures 2A-2F illustrate 2D contour, 3D surface, and perturbation plots to visualize factor effects.

Optimization and validation

The selection of an optimized formulation for any pharmaceutical or biotechnological application is a critical process that hinges on various criteria, with particular emphasis on the Encapsulation Efficiency (%EE) and particle size. In this regard, the criteria for selection of an optimized formulation were primarily focused on achieving the highest possible values of %EE, specifically targeting values greater than 85%. This threshold is essential as it signifies that a significant portion of the active ingredient is successfully encapsulated within the carrier system, ensuring maximum therapeutic efficacy and minimizing wastage of the active drug, which is vital for both cost-effectiveness and performance in clinical settings. Additionally, the particle size of the formulation plays a crucial role in determining its bio-distribution, absorption, and overall pharmacokinetic profile. It was therefore essential to maintain particle sizes under 250 nm, as this range is often associated with enhanced cellular uptake and improved stability in biological systems. Formulations within this size range are better suited for crossing biological barriers and achieving targeted delivery, thus facilitating enhanced therapeutic outcomes. The interplay between achieving high %EE and optimal particle size culminates in the development of a formulation that not only maximizes the effectiveness of the active pharmaceutical ingredient but also ensures patient safety and compliance, ultimately leading to improved health outcomes. Therefore, foundational to the selection process is a careful balance of these parameters, which are critical in guiding the formulation development toward a successful and efficacious therapeutic strategy.

Table 2: Particle size and entrapment efficiency of Lapatinib loaded SLN (L_1-L_{13}) as per Box Behnken design.

Formula CODE	Particlesize (nm)	% Entrapment Efficiency
L1	580±0.72	86.3±0.52
L2	236±0.39	87.8±0.65
L3	670±0.28	87.7±0.57
L4	579±0.12	84±0.73
L5	365±0.37	82.8±0.51
L6	699±0.87	86.7±0.58
L7	423±0.45	82.5±0.42
L8	510±3.61	82±0.49
L9	275±0.76	83.5±0.54
L10	441±0.04	83.5±0.63
L11	412±0.86	84.5±0.62
L12	254±0.67	80.5±0.43
L13	417±0.54	82±0.61

The optimized batch (L2) achieved superior performance compared to other 12 formulations (see Table 2), with >87% EE and smallest particle size (236 nm), indicating improved stability and targeting potential.

Evaluation of optimized batch of Lapatinib loaded SLN

Characterization of optimized batch of Lapatinib loaded SLN

FTIR Studies

FTIR spectra of pure drug and optimized formulation were shown in Figures 3A and 3B. Spectra of Lapatinib Shows its characteristic peaks at 3398 cm^{-1} for -NH- (secondary amine) stretching, 1138 cm^{-1} for C-O-C ether stretching, 1046 cm^{-1} for C-F carbon-fluorine stretching, 656 cm^{-1} for C-Cl carbon-chlorine stretching, 1204 cm^{-1} for -S=O stretching, 3029 cm^{-1} for aromatic =CH stretching. Same peaks are observed in the optimized formulation indicates the compatibility between drug and excipients. The preservation of these peaks suggests that the Lapatinib retains its chemical integrity and that no significant interactions negatively affecting its properties occur during the formulation process. Overall, the FTIR analysis validates that the optimized formulation is effective in maintaining the essential characteristics of Lapatinib, which is crucial for its therapeutic efficacy.

DSC Studies

DSC thermograms of pure drug and optimized formulation were shown in Figures 3C and 3D. From Compatibility studies of lapatinib SLNs there observed a sharp endothermic peak at 114°C and same was observed in the optimized formulation showing no deviation and other excipients have also shown no deviation which means that there is no impurity. This lack of deviation is crucial as it implies that these excipients were compatible with lapatinib and did not react adversely during the formulation process. Overall, the DSC analysis strongly supports the hypothesis that the optimized formulation is pure, stable, and free from impurities, thereby affirming its potential for further development and application in therapeutic settings.

XRD Studies

XRD Studies shown to compatibility with drug as well as other excipients X-ray diffractogram showed multiple peaks for Lapatinib, indicating crystalline nature of drug (Figure 3E). However, X-ray diffractogram of SLNs (Figure 3F) showed diffused spectra without any characteristic peaks of Lapatinib. The crystalline peaks of Lapatinib were absent in SLNs indicating

that the drug was not in crystalline form. This significant change in the diffraction pattern implies that Lapatinib may exist in an amorphous or molecularly dispersed state in the SLNs. Such a transformation could influence the drug's solubility and bioavailability, potentially leading to improved therapeutic efficacy. The results from the XRD studies underscore the importance of understanding the physical form of the drug when developing nanoparticle formulations, as it directly impacts the drug's compatibility with excipients and its overall performance in pharmaceutical applications.

Particle size analysis and Poly Dispersity Index (PDI)

The optimized formulation demonstrates a commendable particle size of 236±0.39 nm, signifying a fine level of precision and consistency in its dimensions. This is coupled with an impressive entrapment efficiency of 87.9±0.65%. Such high efficiency suggests that a significant proportion of the active ingredient is successfully incorporated within the lipid nanoparticles, which is crucial for ensuring the therapeutic effectiveness of the formulation. These measured parameters closely align with the predicted values, indicating that the formulation process was successful and effective in achieving the desired characteristics. To provide a visual representation of the particle size distribution, the curve for the optimized batch of Lapatinib-Solid Lipid Nanoparticles (SLN) is illustrated in Figure 3G. This figure is essential as it offers further insights into the uniformity and distribution of particle sizes within the formulation, which can impact both the pharmacokinetics and overall performance of the delivery system. The data presented suggests that the optimized formulation is well-suited for its intended pharmaceutical application, potentially enhancing the bioavailability and therapeutic outcomes of Lapatinib in clinical settings.

Zeta potential

Research has demonstrated that zeta potentials that exceed ±30 mV are indicative of complete electrostatic stabilization within colloidal systems. This level of zeta potential is critical because it helps to prevent particles from aggregating, thereby ensuring that they remain well-dispersed and stable over time. In the context of our study, the zeta potential of the optimized Solid Lipid Nanoparticle (SLN) formulation for Lapatinib was specifically measured at -43.3 mV, as illustrated in Figure 3H. This value is notably higher than the minimum threshold of ±30 mV, which suggests that it is not only sufficient but also highly effective in maintaining the stability of the SLN formulation. The negative zeta potential implies that the particles carry a negative charge, which fosters repulsion between them, ultimately contributing to their enhanced stability in suspension. Therefore, our findings confirm that the optimized Lapatinib-SLN formulation exhibits excellent electrostatic stabilization characteristics, which is crucial for its potential application in drug delivery systems.

The optimized Solid Lipid Nanoparticles (SLNs) exhibited a particle size of ~236 nm, a low PDI, and a zeta potential of -43.3 mV, all of which are crucial for effective tumor targeting and formulation stability. The particle size falls within the ideal range for passive accumulation in tumor tissues via the Enhanced Permeation and Retention (EPR) effect, where leaky vasculature allows nanoparticles to preferentially localize in tumor sites. A low PDI indicates a uniform size distribution, ensuring consistent biodistribution and reduced aggregation. The high negative zeta potential provides strong electrostatic repulsion between particles, enhancing colloidal stability and preventing aggregation during circulation. Additionally, the negative charge reduces opsonization and clearance by macrophages, prolonging systemic circulation and improving the therapeutic window.

SEM Studies

Spherical particles possess a unique characteristic of symmetry in all three dimensions, which significantly enhances their ability to be transported across epithelial tissues when compared to ellipsoidal particles. This inherent three-dimensional symmetry enables spherical particles to navigate through the complex

Table 3: Results of the statistical analysis concerning particle size and entrapment efficiency.

Parameter	Particlesize (Y1)		Entrapment efficiency (Y2)	
	Coefficient	*p*-value	Coefficient	*p*-value
K	+511.96	0.066	+79.00	0.062
A	+36.53	0.06	+09.000	0.081
B	-65.94	0.08	-0.112	0.089
C	-39.89	0.074	+0.58	0.049
D	+36.46	0 .0623	+0.99	0.0599
E	-161.37	0.0039*	-2.01	0.0171*
F	+73.68	0.0341*	+2.82	0.0051*
G	+39.19	0.2103	+1.201	0.101
H	-93.27	0.0358*	+0.099	0.0789
I	-29.93	0.03321*	+2.312	0.0201*

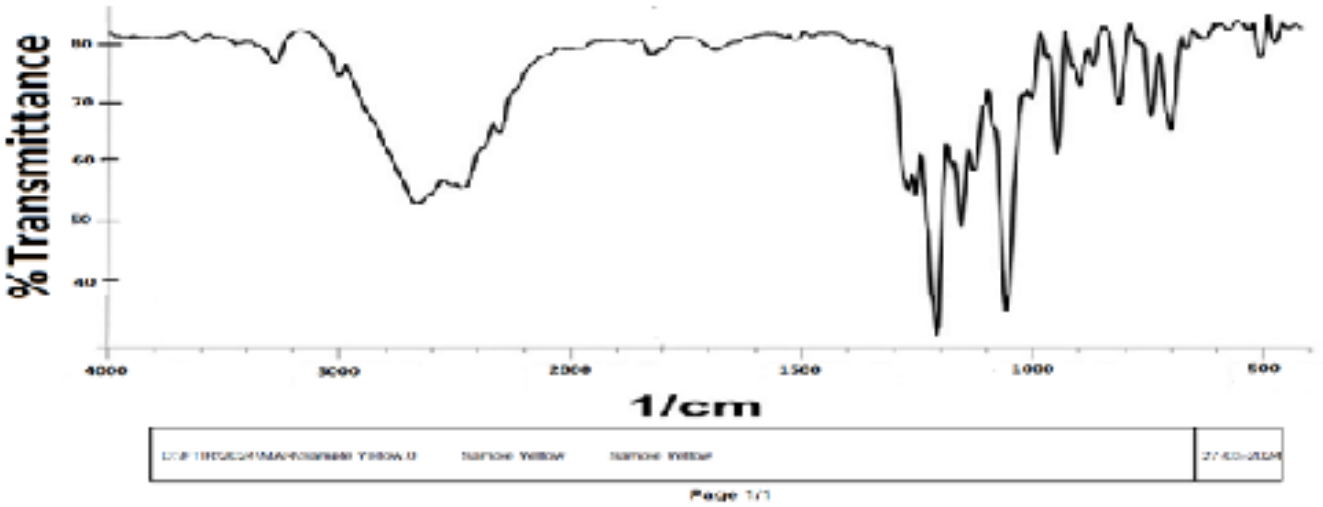
%Transmittance
80
70
60
50
40
4000
3000
2000
1500
1000
500
1/cm
Page 1/1

3A

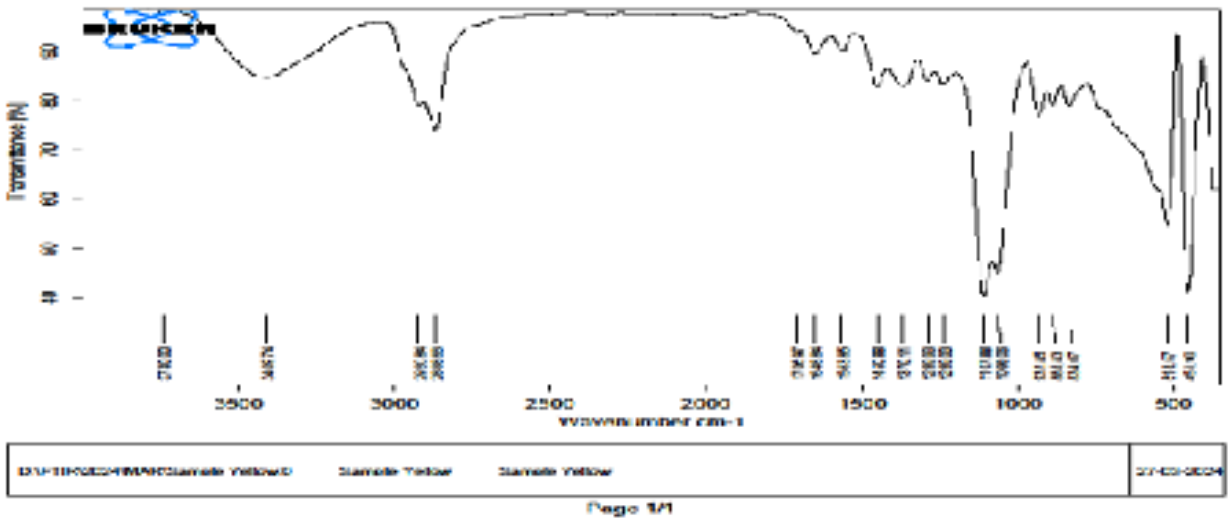
Transmittance (%)
90
80
70
60
50
3500
3000
2500
2000
1500
1000
500
Page 1/1

3B

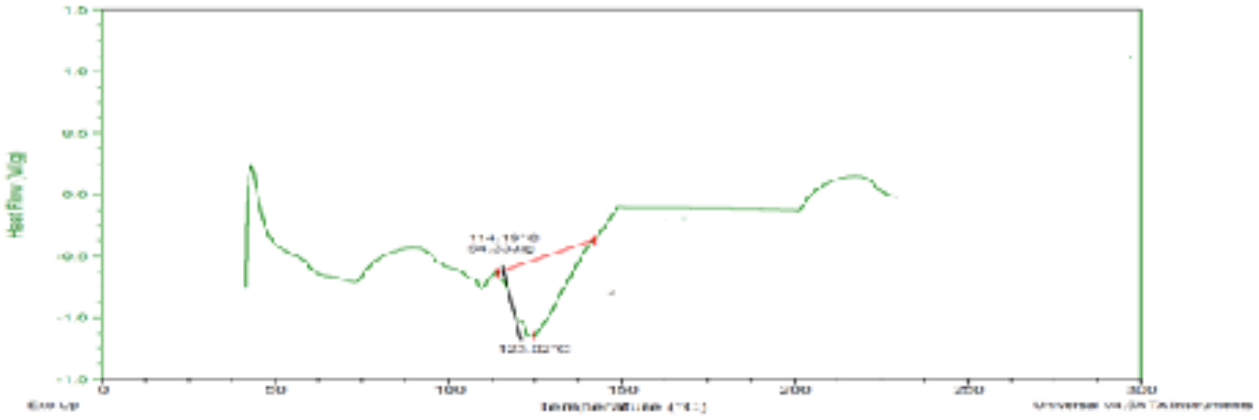
Heat Flow W/g
1.5
1.0
0.5
0.0
-0.5
-1.0
-1.5
0
50
100
150
200
250
300
Exo Up

3C

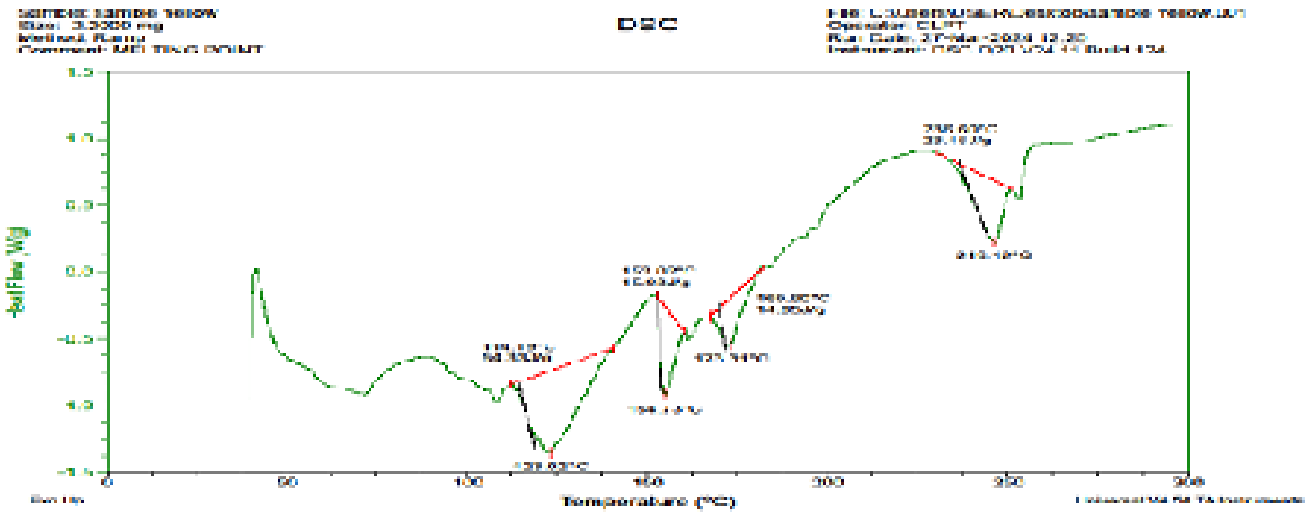

3D

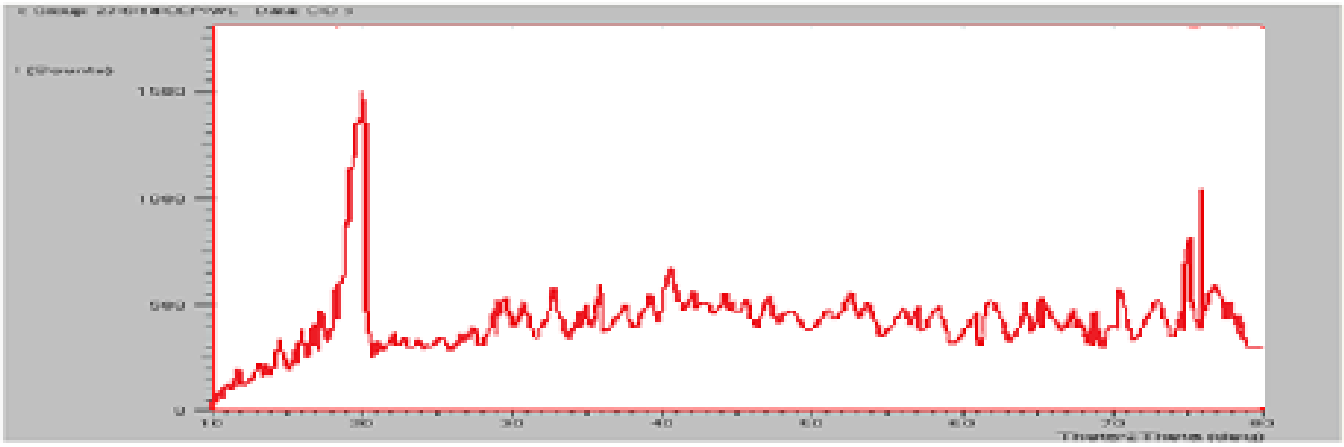

3E

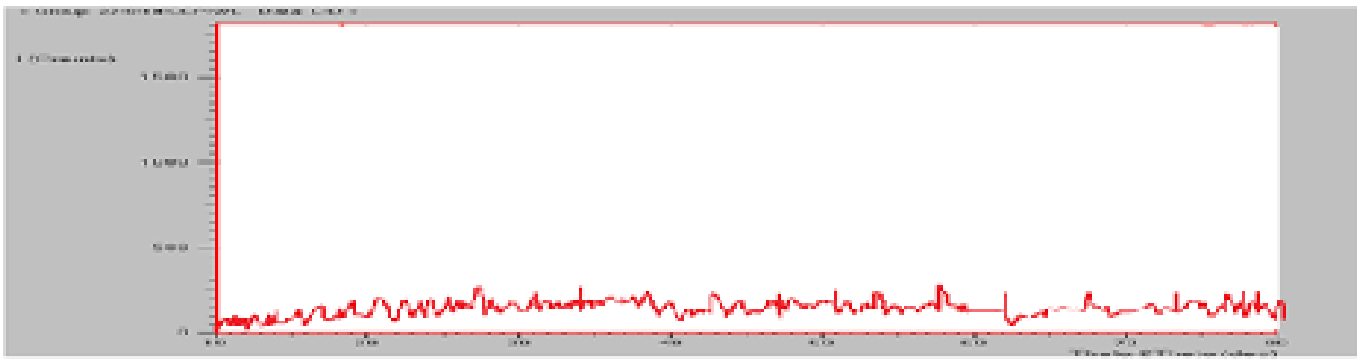

3F

Results

		Size (d.n...	% Intensity:	St Dev (d.n...
Z-Average (d.nm): 235	Peak 1:	246	100.0	0.39
PdI: 0.610				

Result quality Good

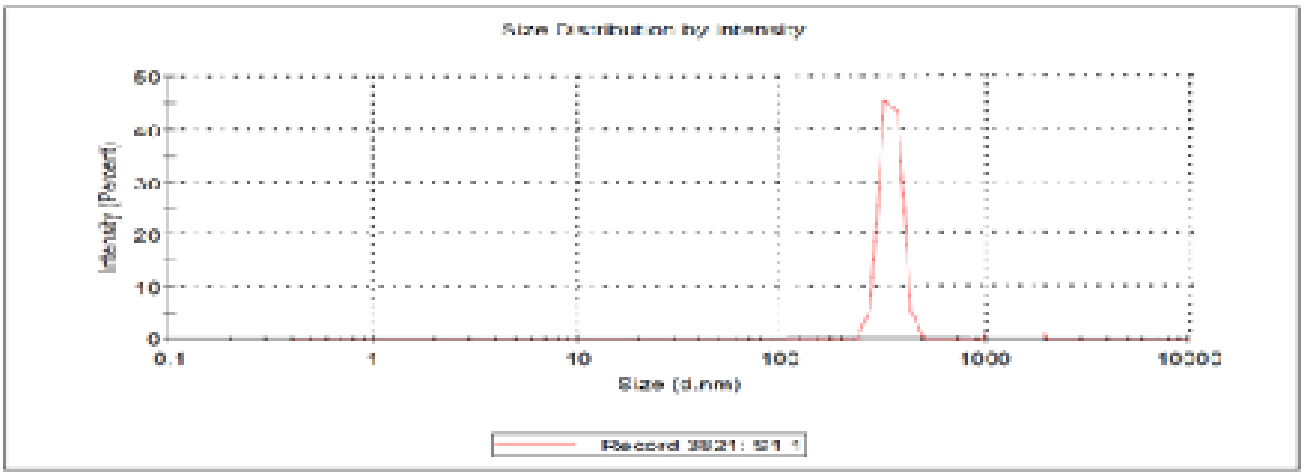

3G

System

Temperature (°C):	25.0	Zeta Runs:	10
Count Rate (kcps):	24.0	Measurement Position (mm):	4.50
Cell Description:	Zeta dip cell	Attenuator:	7

Results

		Mean (mV)	Area (%)	St Dev (mV)
Zeta Potential (mV): -43.3	Peak 1:	-42.7	100.0	9.82
Zeta Deviation (mV): 9.92	Peak 2:	0.00	0.0	0.00
Conductivity (mS/cm): 0.036	Peak 3:	0.00	0.0	0.00

Result quality See result quality report

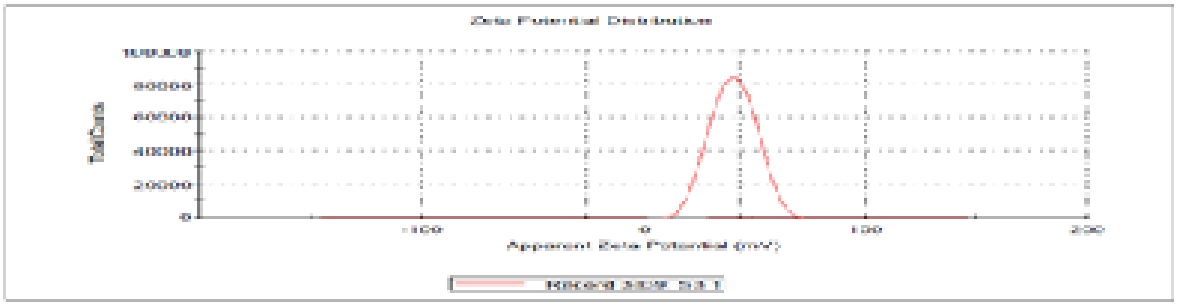

3H

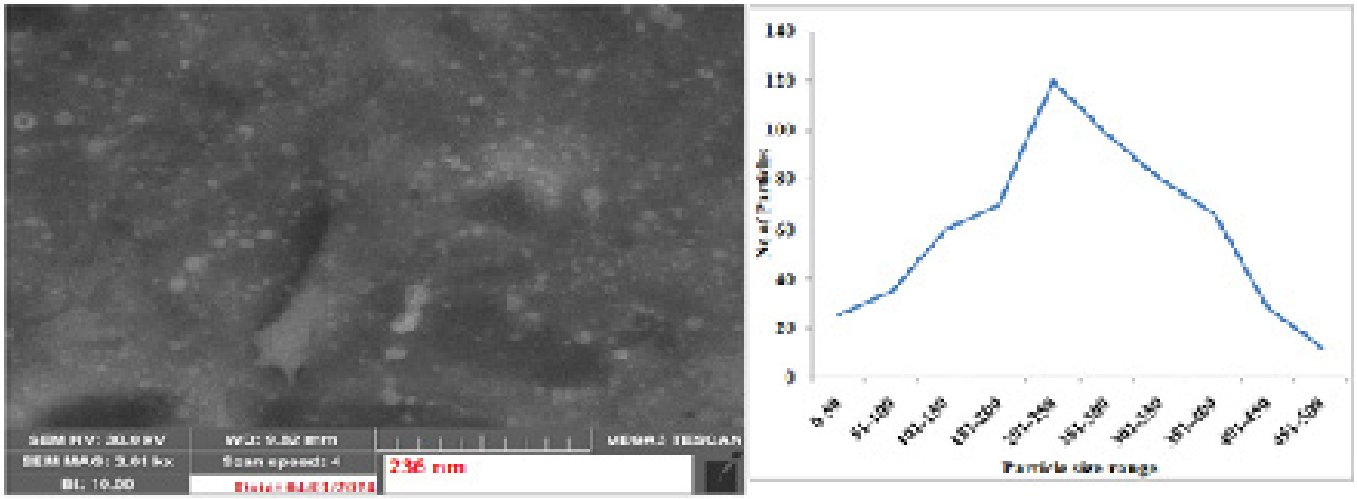

3I

Figure 3: 3A-FTIR Spectra of pure drug, 3B-FTIR Spectra of Optimized Formulation, 3C-DSC of pure drug, 3D-DSC of Optimized Formulation, 3E-XRD patterns of Pure Drug, 3F-XRD patterns of Optimized Formulation, 3G-Particle size analysis and Poly Dispersity Index (PDI) of optimized formulation of Lapatinib loaded SLN, 3F-Zeta potential of optimized formulation of Lapatinib loaded SLN and 3I-SEM Photograph optimized formulation of Lapatinib loaded SLN.

microenvironment of epithelial layers more efficiently, allowing them to move without encountering excessive friction or resistance. In a recent study, the Scanning Electron Microscope (SEM) image provided compelling visual evidence of the Solid Lipid Nanoparticles (SLN) under investigation. The image revealed that these nanoparticles exhibited a well-defined and uniform size, with each particle adopting a distinctly spherical shape. This uniformity in size and shape is crucial for ensuring consistent behavior during interactions with biological barriers, as illustrated in Figure 3I. The well-defined morphology of the SLNs not only facilitates their transport across epithelial surfaces but also suggests their potential for effective drug delivery applications, as they can be formulated in a way that optimizes bioavailability and therapeutic efficacy.

In vitro Evaluations *in vitro* drug release study

The *in vitro* release study of the LP-SLNs was conducted using the dialysis bag technique. To ensure sink conditions were maintained, Tween®80 (0.5%) was included in the release medium. The LP so released from the formulation was quantified using a HPLC. The CPR was calculated and the release profile was plotted between % CPR and time. Various kinetic models were employed to analyze the data from the release studies, revealing that the release of LP from SLNs adhered to the Higuchi model provided the best fit, with an R2 >0.99. Additionally, the Peppas exponent n was determined to be 0.477, indicating that the LP release was governed by Fick's diffusion indicative of sustained and controlled release in tumor microenvironments. The *in vitro* drug release pattern of the formulation was studied at two different pH conditions simulating the different biological sites through which the formulation was expected to come in contact with. The selected media was pH 7.4 and pH 5.0, which is the pH of the blood and the tumour environment, respectively. During the initial period, the rate of drug release from same formulation at two different pH were similar, while a significant difference (p<0.001) in cumulative drug release was witnessed after 4 hr. The drug release slowed down during the second stage which is characterized by flattening of the curve of release profile where in the entrapped drug was slowly released from the micellar structure. The drug release rate from the formulations was higher at pH 5.0 compared to pH 7.4. This finding suggests that the LP-SLNs could potentially provide a more efficient drug release profile in tumor environments, thereby enhancing the therapeutic efficacy of the formulation in targeting cancerous tissues. Overall, these results underline the importance of pH-dependency in the design and application of drug delivery systems, particularly in formulations intended for targeted therapy in diverse biological contexts.

In vitro screening of anti-cancer efficacy

Cell Culture

In vitro evaluation of the anticancer efficacy was carried out using SKBr3 breast cancer cell line because of its characteristic feature/ability to over express HER2 and can serve as best for the present study Cytotoxicity assay.

Percent cell viability after treatment with various concentrations of LP and LP-SLNs is graphically illustrated in Figure 4A. LP-SLNs (IC_{50}:1.60 µg/mL) and had shown better anticancer efficacy over LP only (IC_{50}-8.19 µg/mL). The results indicated that the LP-SLNs possessed better anti-cancer activity than the free drug against the cell lines.

LP causes the arrest in growth of tumor cell lines that express EGFR and HER2. It binds reversibly to the ATP-binding site of the kinase domain of EGFR and HER2 to prevent auto phosphorylation. Thus, LP exhibits antagonistic activity against EGFR and HER2. The cell toxicity/ anti-cancer activity of the formulation was evaluated by the MTT-based assay on SKBr3 breast cancer cell line. The activity is being measured in terms of IC_{50} value which represents the concentration of a drug required to inhibition of cell growth by 50% in comparison to controls.

MTT assay results suggested that LP-SLNs inhibits the HER2 expressing cancer cell lines as the IC_{50} values of LP-SLNs against SKBr3 cell line were significantly lower compared to LP treated SKBr3 cell line. The IC_{50} of LP-SLNs was lower by almost 6 folds against SKBr3 in comparison to LS, which indicated the greater anti-cancer efficacy of LP-SLNs. In summary, the findings from this study provide compelling evidence that the formulation of LP within solid lipid nanoparticles significantly augments its anticancer activity. This suggests that utilizing LP-SLNs may represent a more effective therapeutic strategy for targeting cancers characterized by EGFR and HER2 overexpression, thereby offering a promising avenue for improved cancer treatment regimens.

In vitro anti-cancer efficacy studies

Figure 4B presents a detailed overview of the morphological alterations observed in SKBr3 breast cancer cells upon treatment. Initially, the SKBr3 cells exhibit a cuboidal and polygonal structure, which is indicative of their natural morphology as observed in the Field of Vision (FOV). However, following treatment with Lipid-Based Solid Lipid Nanoparticles (LP-SLNs), significant changes in the cell morphology become evident. The cells transform into a more rounded shape, accompanied by a noticeable reduction in size, as denoted by the marked changes (#). Additionally, there is an observable increase in granular content within the cytoplasm ($), as well as a loss of confluence among the cells (*), suggesting that the cells are no longer adhering to one another as they typically would. In contrast, the cultures treated with free Liposomal Formulation (LS) demonstrated that only a minor proportion of the cells displayed altered morphology, while the majority retained their typical cuboidal and polygonal shapes, indicating a lesser degree of impact from the treatment. To reinforce the assessment of the anti-cancer efficacy of LP encapsulated within the SLNs, a comparison of the morphological alterations instigated by both LP and LP-SLNs treatments was conducted. Notably, in the cultures treated with LP-SLNs, cytoplasmic condensation was prominently observed, leading to a considerable shrinkage of the cells and a shift towards a rounded morphology. Morphological changes such as cell rounding, shrinkage, and granularity suggest apoptosis. These findings suggest that the LP-SLNs induce apoptosis, or programmed cell death, in the cancerous cells. The emergence of a granular structure within the cells could likely be attributed to chromatin condensation and potential fragmentation of the nucleus, both characteristic features of apoptotic cells. Furthermore, the observed morphological changes, along with the significant decrease in the number of viable cells in the LP-SLNs-treated cultures, bolster the assertion that our results are consistent with

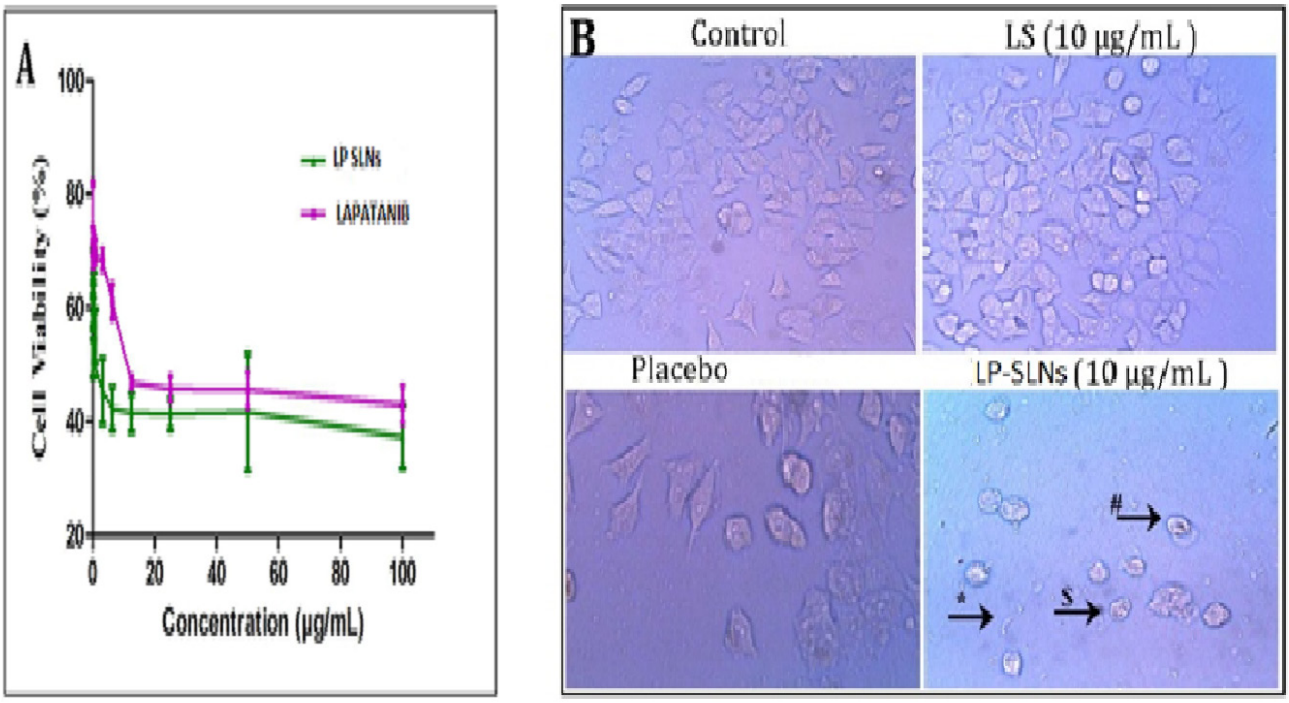

Figure 4: 4A. Cytotoxicity assay of Lapatinib loaded SLN and 4B. *In vitro* anti-cancer efficacy studies.

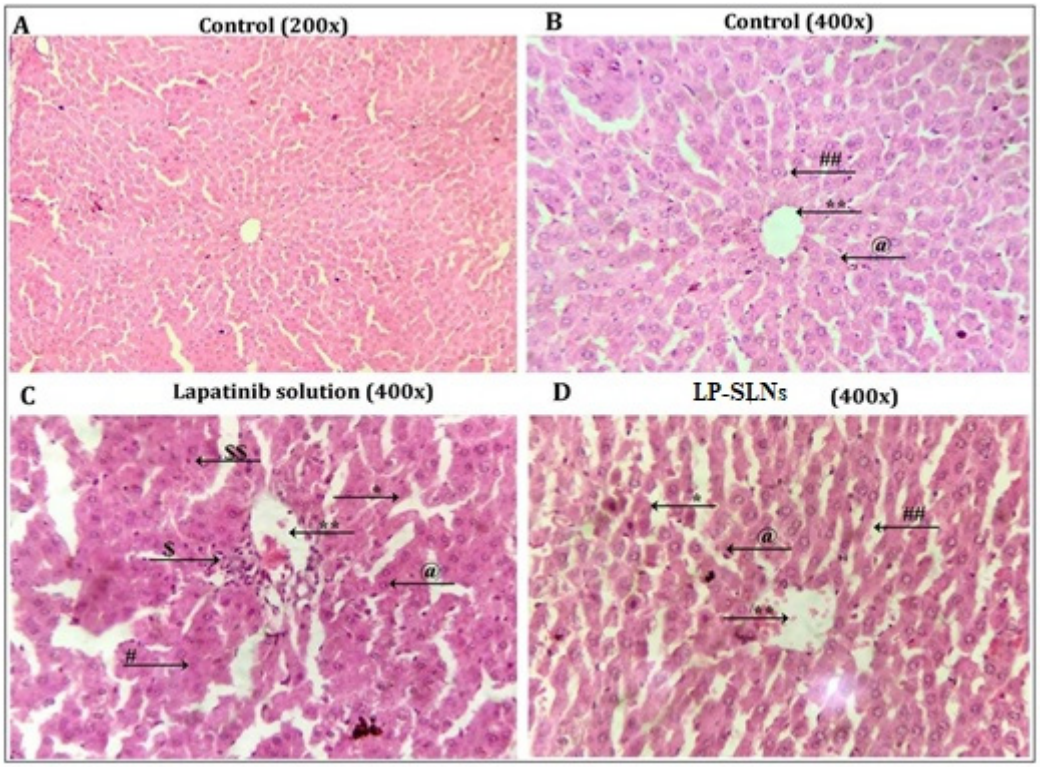

Figure 5: Histopathological Studies.

those reported in previous studies regarding the efficacy of LP encapsulated in SLNs. On the other hand, the decreased cellular activity noted in the LS-treated groups can likely be attributed to the low solubility of the free liposomal formulation, which may limit cellular uptake and consequently attenuate the anti-cancer effects. Interestingly, it is important to note that the placebo micelles demonstrated an absence of cytotoxic activity against the SKBr3 cells, underscoring the specific efficacy of the LP-SLNs in effectively targeting and reducing the viability of breast cancer cells. Overall, these findings contribute to a deeper understanding of the potential therapeutic applications of LP-SLNs in cancer treatment.

Histopathological Studies

Hepatotoxicity is one of the significant side-effect of tyrosine kinase inhibitor family of anti-cancer drugs of which LP is a member. The hepatotoxicity is determined by observing the significant changes in the normal hepatocytic parenchyma of the hepatic lobules. The changes include enlargement or dilatation of sinusoidal spaces, hydropic degeneration, vacuolization of hepatocytes, disruption of lobular organization, infiltration of inflammatory cells like neutrophil as a sign of inflammation, and necrosis, etc. The normal parenchyma of hepatocytes (denotedby@) and converging histological organization of hepatocytes with central vein (denoted by **) that can be seen from Figure (5A and 5B). Additionally, Kupffer cells (denoted by ##) were intermittently scattered and identified by their characteristic spindle shaped nuclei. The group treated with oral lapatinib solution showed significant toxicity to liver as depicted from Figure (5C). It is evidenced by the symptoms like sinusoidal dilatation (denoted by *) and disorganization of hepatocytes and sinusoidal spaces (denoted by #). Also, significant inflammation around central vein was confirmed by the presence inflammatory cells (denoted by $) with fewer hepatocytes undergoing necrosis and degeneration of their nuclei (denoted by $$). Further, as seen from Figure (5D), the absence of most of the toxicity symptoms except milder dilatation of sinusoidal spaces in perilobular space revealed that the LP-SLNs were safe as compared to lapatinib solution; however very milder hepatotoxicity did exist comparing to normal liver. The pharmacokinetics of lapatinib indicate that it is primarily metabolized by liver enzymes CYP3A4 and CYP3A5. During this metabolic process, LP forms various metabolites, predominantly dealkylated phenolic metabolites, which have been implicated in hepatotoxicity as reported by Spraggs *et al.* (2013). Following oral administration, LP passes through the gastrointestinal tract and enters the portal circulation, leading to substantial exposure of the liver to the compound since a considerable portion of the absorbed LP reaches the liver. This pathway significantly contributes to the liver's maximum exposure and the resultant hepatotoxicity. A key objective of the study was to mitigate the liver's exposure to lapatinib by utilizing intravenous (I.V.) administration instead. Additionally, encapsulating the drug within the core of the lapatinib-stabilized lipid nanoparticles could considerably lower the concentration of unbound LP in the bloodstream that circulates through the liver. This innovative approach is supported by the findings illustrated

in Figure 5D, which indicate a marked reduction in liver toxicity associated with the encapsulated formulation compared to the traditional oral lapatinib solution.

CONCLUSION

The successful development and optimization of Solid Lipid Nanoparticles (SLNs) formulations loaded with the anti-cancer drug Lapatinib was achieved through the use of a technique known as probe sonication, combined with a statistical approach called Box-Behnken design. This meticulous process led to the creation of a highly effective formulation that showcases several advantageous characteristics. Firstly, the SLNs demonstrated remarkable entrapment efficiency, meaning that a significant amount of the Lapatinib was successfully retained within the lipid nanoparticles, preventing it from being released prematurely. Secondly, the size of the particles produced was in the nanometer range, which is critical for enhancing drug delivery and ensuring that the formulation can penetrate biological barriers effectively. Moreover, the zeta potential of the formulation was found to be favorable, indicating good stability and reduced likelihood of aggregation in solution. This stability is crucial for maintaining the integrity of the nanoparticles during storage and administration. The implications of these advancements are significant in the context of cancer treatment. The formulation not only enhances the anti-cancer efficacy of Lapatinib but also plays a crucial role in reducing liver toxicity. By minimizing the circulation of free Lapatinib in the bloodstream, the risk of side effects associated with the drug can be considerably lowered. This targeted delivery mechanism is especially pertinent given that many cancer therapies can exert considerable stress on the liver and other organs. Additionally, the SLNs exhibit the potential to function as a sustained release drug delivery system. This characteristic is particularly beneficial in targeting the acidic microenvironment often found in tumors, allowing for a more controlled and prolonged release of Lapatinib directly at the site of action. This specificity not only maximizes the therapeutic effects on cancer cells but also further minimizes systemic side effects, enhancing the overall safety and efficacy of the treatment. In conclusion, the development of these optimized SLN formulations represents a significant advancement in drug delivery systems for cancer therapy, combining improved therapeutic efficacy, reduced toxicity, and the ability for sustained release system targeting the acidic environment of tumors, thereby offering promising prospects for future applications in oncology.

ACKNOWLEDGEMENT

The authors would like to thank A. M. Reddy Memorial College of Pharmacy and K. L. College of Pharmacy (KLU) for providing support to perform this work.

ABBREVIATIONS

SLN: Solid Lipid Nanoparticles; **LP:** Lapatinib; **EE:** Encapsulation Efficiency; **PSD:** Particle Size Distribution; **IC_{50}:** Half Maximal Inhibitory Concentration; **HPLC:** High-Performance Liquid Chromatography; **PBS:** Phosphate-Buffered Saline; **CPR:** Cumulative percentage release.

CONFLICT OF INTEREST

The authors declare that there is no conflict of interest.

AUTHOR'S CONTRIBUTIONS

R. Sunitha was responsible for the conduction of the experimental work, collection and integration of data, and drafting the manuscript, while dr. Praveen Sivadasu provided supervision, visualization, and critical manuscript review and editing; Dr. P. Bhargava Bhushan Rao and Dr. Raghavendra Kumar Gunda contributed by formulating the study hypothesis and methodology, overseeing the research process, interpreting the data, and enhancing the manuscript through his reviewing and editing expertise.

SUMMARY

This study evaluates Lapatinib-loaded SLNs for targeted breast cancer treatment. The formulation was optimized using the Box-Behnken design. Results demonstrated high encapsulation efficiency (>85%), particle size under 250 nm, and enhanced drug release in the acidic tumor microenvironment. *In vitro* studies confirmed significantly improved anticancer efficacy. Histopathological findings indicated reduced liver toxicity. These results suggest that SLNs offer a promising platform for enhancing the therapeutic effectiveness of anticancer agents.

REFERENCES

1. World Health Organization. Global Health Observatory. [Internet]. [cited 2020 Nov 1]. Available from:https://gco.iarc.fr/today/data/factsheets/cancers/39-All-cancers-fact-sheet.pdf
2. World Health Organization. Global Health Observatory. [Internet]. [cited 2020 Nov 1]. Available from:https://gco.iarc.fr/tomorrow/home
3. National Institute of Health, National Cancer Institute. [Internet]. [cited 2020 Nov 1]. A vailable from:https://www.cancer.gov/about-cancer/treatment/types/
4. Chidambaram M, Manavalan R, Kathiresan K. Nanotherapeutics to overcome conventional cancer chemotherapy limitations. J Pharm Pharm Sci. 2011;14(1):67-77. doi: 10.18433/j30c7d.
5. Li J, Chen F, Cona MM, Feng Y, Himmelreich U, Oyen R, *et al.* A review on various targeted anticancer therapies. Target Oncol. 2012;7(1):69-85. doi: 10.1007/s11523-012-0212-2.
6. Bhullar KS, Lagarón NO, McGowan EM, Parmar I, Jha A, Hubbard BP, *et al.* Kinase-targeted cancer therapies: progress, challenges and future directions. Mol Cancer. 2018;17(1):48. doi: 10.1186/s12943-018-0804-2.
7. Herbrink M, Nuijen B, Schellens JH, Beijnen JH. Variability in bioavailability of small molecular tyrosine kinase inhibitors. Cancer Treat Rev. 2015;41(5):412-22. doi: 10.1016/j.ctrv.2015.03.005.
8. Dadwal A, Baldi A, Kumar Narang R. Nanoparticles as carriers for drug delivery in cancer. Artif Cells Nanomed Biotechnol. 2018;46(Suppl 2):295-305. doi: 10.1080/21691401.2018.1457039.
9. Parhi R, Suresh P. Preparation and characterization of solid lipid nanoparticles—a review. Curr Drug Discov Technol. 2012;9(1):2-16. doi: 10.2174/157016312799304552.

10. Moradpour Z, Barghi L. Novel approaches for efficient delivery of tyrosine kinase inhibitors. J Pharm Pharm Sci. 2019;22(1):37-48. doi: 10.18433/jpps29891.
11. Josephs DH, Fisher DS, Spicer J, Flanagan RJ. Clinical pharmacokinetics of tyrosine kinase inhibitors: implications for therapeutic drug monitoring. Ther Drug Monit. 2013;35(5):562-87. doi: 10.1097/FTD.0b013e318292b931.
12. Di Gion P, Kanefendt F, Lindauer A, Scheffler M, Doroshyenko O, Fuhr U, *et al.* Clinical pharmacokinetics of tyrosine kinase inhibitors: focus on pyrimidines, pyridines and pyrroles. Clin Pharmacokinet. 2011;50(9):551-603. doi: 10.2165/11593320-000000000-00000.
13. Ferguson FM, Gray NS. Kinase inhibitors: the road ahead. Nat Rev Drug Discov. 2018;17(5):353-77. doi: 10.1038/nrd.2018.21.
14. Roskoski R Jr. Properties of FDA-approved small molecule protein kinase inhibitors: a 2020 update. Pharmacol Res. 2020;152:104609. doi: 10.1016/j.phrs.2019.104609.
15. Aisner J. Overview of the changing paradigm in cancer treatment: oral chemotherapy. Am J Health Syst Pharm. 2007; 64(9 Suppl 5):S4-7. https://doi.org/10.2146/ajhp070035.
16. Rowland A, van Dyk M, Mangoni AA, Miners JO, McKinnon RA, Wiese MD, *et al.* Kinase inhibitor pharmacokinetics: comprehensive summary and roadmap for addressing inter-individual variability in exposure. Expert Opin Drug Metab Toxicol. 2017; 13(1): 31-49. https://doi.org/10.1080/17425255.2016.1229303.
17. Yu H, Steeghs N, Nijenhuis CM, Schellens JH, Beijnen JH, Huitema AD. Practical guidelines for therapeutic drug monitoring of anticancer tyrosine kinase inhibitors: focus on the pharmacokinetic targets. Clin Pharmacokinet. 2014;53(4):305-25. https://doi.org/10.1007/s40262-014-0137-2.
18. Kumar S, Bhargava D, Thakkar A, Arora S. Drug carrier systems for solubility enhancement of BCS class II drugs: a critical review. Crit Rev Ther Drug Carrier Syst. 2013; 30(3): 217-56. https://doi.org/10.1615/critrevtherdrugcarriersyst.2013005964.
19. Bachovchin KA, Sharma A, Bag S, Klug DM, Schneider KM, Singh B, *et al.* Improvement of aqueous solubility of lapatinib-derived analogues: identification of a quinolinimine lead for human African trypanosomiasis drug development. J Med Chem. 2019;62(2):665-687. https://doi.org/10.1021/acsmedchemlett.9b00455.
20. Mondal S, Biswal S, Acharya T, Mondal P, Bhar K. Determination of lapatinib in bulk and tablet dosage form using ultraviolet spectrophotometric and RP-HPLC analytical methods. Int J Pharm Investig. 2021; 11(2): 208-13. https://doi.org/DOI:10.5530/ijpi.2021.2.37.
21. Katolkar P, Gaydhane N, Vidhate S, Gatterwar A, Motghare A, Baheti J. Analytical method development and validation for estimation of lapatinib in formulation by RP-HPLC with stability indicating. Res J Pharm Technol. 2023;16(7):3215-21. https://doi.org/10.52711/0974-360X.2023.00514.
22. Kumar K, Nagoji K, Nadh R. A validated RP-HPLC method for the estimation of lapatinib in tablet dosage form using gemcitabine hydrochloride as an internal standard. Indian J Pharm Sci. 2012; 74(6): 580-583. doi: 10.4103/0250-474X.110621 .*(Added page numbers as indicated by the DOI results)*
23. Sparreboom A, de Bruijn P, Nooter K, Loos WJ, Stoter G, Verweij J. Determination of paclitaxel in human plasma using single solvent extraction prior to isocratic reversed-phase high-performance liquid chromatography with ultraviolet detection. J Chromatogr B. 1998;705(1-2):159-64. doi: 10.1016/S0378-4347(97)00502-1.
24. Satapathy S, Patro CS. Solid lipid nanoparticles for efficient oral delivery of tyrosine kinase inhibitors: a nano-targeted cancer drug delivery. Adv Pharm Bull. 2022; 12(2): 298-308. https://doi.org/10.34172/apb.2022.041.
25. Swidan S, Ghonaim H, Samy A, Ghorab ME. Efficacy and *in vitro* cytotoxicity of nanostructured lipid carriers for paclitaxel delivery. J Appl Pharm Sci. 2016;6:18-26. https://doi.org/10.7324/JAPS.2016.60903.
26. Khare A, Singh I, Pawar P, Grover K. Design and evaluation of voriconazole loaded solid lipid nanoparticles for ophthalmic application. J Drug Deliv. 2016; 2016: 6590361. doi: 10.1155/2016/6590361.
27. Cao X, Luo J, Gong T, Zhang ZR, Sun X, Fu Y. Coencapsulated doxorubicin and bromotetrandrine lipid nanoemulsions in reversing multidrug resistance in breast cancer *in vitro* and *in vivo*. Mol Pharm. 2015;12:274-86. doi: 10.1021/mp500637b.
28. Eljack S, David S, Chourpa I, Faggad A, Allard-Vannier E. Formulation of lipid-based nanoparticles for simultaneous delivery of lapatinib and anti-survivin siRNA for HER2+ breast cancer treatment. Pharmaceuticals. 2022; 15(12): 1452. doi: 10.3390/ph15121452.
29. Qushawy M, Prabahar K, Abd-Alhaseeb M, Swidan S, Nasr A. Preparation and evaluation of carbamazepine solid lipid nanoparticle for alleviating seizure activity in pentylenetetrazole-kindled mice. Molecules. 2019;24:3971. doi: 10.3390/molecules24213971.
30. Hao J, Fang X, Zhou Y, Wang J, Guo F, Li F, *et al.* Development and optimization of solid lipid nanoparticle formulation for ophthalmic delivery of chloramphenicol using a Box-Behnken design. Int J Nanomedicine. 2011;6:683-92. doi: 10.2147/IJN.S17386.
31. Singh AK, Mukerjee A, Pandey H, Mishra SB. Fabrication of solid lipid nanoparticles by hot high shear homogenization and optimization by Box-Behnken design: An accelerated stability assessment. J Appl Pharm Sci. 2021;11(09):035-47. https://doi.org/10.7324/JAPS.2021.110905.
32. Kumar SK, Narayan R, Ahammed V, Nayak Y, Naha A, Nayak U. Development of ritonavir solid lipid nanoparticles by Box Behnken design for intestinal lymphatic targeting. J Drug Deliv Sci Technol. 2018; 44(4): 181-9. doi: 10.1016/j.jddst.2017.12.014.
33. Klaus B. Statistical relevance—relevant statistics, part I. EMBO J. 2015;34(22):2727-30. doi: 10.15252/embj.201592958.
34. Stella B, Peira E, Dianzani C, Gallarate M, Battaglia L, Gigliotti CL, *et al.* Development and characterization of solid lipid nanoparticles loaded with a highly active doxorubicin derivative. Nanomaterials (Basel). 2018; 8(2): 110. doi: 10.3390/nano8020110.
35. Mehnert W, Mäder K. Solid lipid nanoparticles: Production, characterization and applications. Adv Drug Deliv Rev. 2012;64(1):83-101. doi: 10.1016/j.addr.2012.09.021.
36. Andonova V, Peneva P. Characterization methods for solid lipid nanoparticles (SLN) and nanostructured lipid carriers (NLC). Curr Pharm Des. 2017;23(20):3661-74. doi: 10.2174/1381612823666171115105721.
37. Alamri A, Alqahtani A, Alqahtani T, Al Fatease A, Asiri SA, Gahtani RM, *et al.* Design, physical characterizations, and biocompatibility of cationic solid lipid nanoparticles in HCT-116 and 16-HBE cells: A preliminary study. Molecules. 2023;28(4):1711. doi: 10.3390/molecules28041711.
38. Reddy LH, Vivek K, Bakshi N, Murthy RSR. Tamoxifen citrate loaded solid lipid nanoparticles (SLN™): Preparation, characterization, *in vitro* drug release, and pharmacokinetic evaluation. Pharm Dev Technol. 2006;11(2):167-77. doi: 10.1080/10837450600561265.
39. Kumar S, Bajaj S, Bodla RB. Preclinical screening methods in cancer. Indian J Pharmacol. 2016;48(5):481-6. doi: 10.4103/0253-7613.190716.
40. Baksi R, Singh DP, Borse SP, Rana R, Sharma V, Nivsarkar M. *In vitro* and *in vivo* anticancer efficacy potential of Quercetin loaded polymeric nanoparticles. Biomed Pharmacother. 2018;106:1513-26. doi: 10.1016/j.biopha.2018.07.106.
41. Kabir MF, Ullah AKMA, Ferdousy J, *et al.* Anticancer efficacy of biogenic silver nanoparticles *in vitro*. SN Appl Sci. 2020; 2: 1111. doi: 10.1007/s42452-020-2929-3.
42. Valizadeh A, Khaleghi AA, Roozitalab G, Osanloo M. High anticancer efficacy of solid lipid nanoparticles containing Zataria multiflora essential oil against breast cancer and melanoma cell lines. BMC Pharmacol Toxicol. 2021 Sep 30;22(1):52. doi: 10.1186/s40360-021-00523-9.
43. Wang W, Chen T, Xu H, Ren B, Cheng X, Qi R, *et al.* Curcumin-Loaded Solid Lipid Nanoparticles Enhanced Anticancer Efficiency in Breast Cancer. Molecules. 2018;23(7):1578. doi: 10.3390/molecules23071578.
44. Parvez S, Karole A, Mudavath SL. Fabrication, physicochemical characterization, and *in vitro* anticancer activity of nerolidol encapsulated solid lipid nanoparticles in human colorectal cell line. Colloids Surf B Biointerfaces. 2022;215:112520. doi: 10.1016/j.colsurfb.2022.112520.
45. Gurcan MN, Boucheron LE, Can A, Madabhushi A, Rajpoot NM, Yener B. Histopathological image analysis: a review. IEEE Rev Biomed Eng. 2009;2:147-71. doi: 10.1109/RBME.2009.2034865.
46. Hamishehkar H, Shokri J, Fallahi S, Jahangiri A, Ghanbarzadeh S, Kouhsoltani M. Histopathological evaluation of caffeine-loaded solid lipid nanoparticles in efficient treatment of cellulite. Drug Dev Ind Pharm. 2014;41(10):1640-6. doi: 10.3109/03639045.2014.980426.
47. Jia Y, Ji J, Wang F, Shi L, Yu J, Wang D. Formulation, characterization, and *in vitro/vivo* studies of aclacinomycin A-loaded solid lipid nanoparticles. Drug Deliv. 2014;23(4):1317-25. doi: 10.3109/10717544.2014.974001.
48. Khames A, Khaleel MA, El-Badawy MF, El-Nezhawy AOH. Natamycin solid lipid nanoparticles - sustained ocular delivery system of higher corneal penetration against deep fungal keratitis: preparation and optimization. Int J Nanomedicine. 2019;14:2515-31. doi: 10.2147/IJN.S190502.
49. Madane RG, Mahajan HS. Curcumin-loaded nanostructured lipid carriers (NLCs) for nasal administration: design, characterization, and *in vivo* study. Drug Deliv. 2014;23(4):1326-34. doi: 10.3109/10717544.2014.975382.
50. García-Moreno E, Gascón S, García de Jalón JA, Romanos E, Rodriguez-Yoldi MJ, Cerrada E, *et al. In Vivo* Anticancer Activity, Toxicology and Histopathological Studies of the Thiolate Gold(I) Complex [Au(Spyrimidine)(PTA-CH2Ph)]Br. Anticancer Agents Med Chem. 2015;15(6):773-82. doi: 10.2174/1871520615666150129211440.

Cite this article: Sunitha R, Sivadasu P, Rao PBB, Gunda RK. Optimizing Tumor-Targeting Drug Delivery of Potent Anti-Cancer Drug Using Doe-Guided Solid Lipid Nanoparticle Formulation: *In vitro* Cell Line Studies and Histopathological Analysis. Indian J of Pharmaceutical Education and Research. 2026;60(2s):s776-s793.